North Pacific seasonality and the glaciation of North America 2.7 million years ago

Gerald H. Haug[1], Andrey Ganopolski[2], Daniel M. Sigman[3], Antoni Rosell-Mele[4], George E. A. Swann[5], Ralf Tiedemann[6], Samuel L. Jaccard[7], Jörg Bollmann[7], Mark A. Maslin[5], Melanie J. Leng[8] & Geoffrey Eglinton[9]

[1]*Geoforschungszentrum Potsdam (GFZ), and* [2]*Potsdam Institute for Climate Impact Research (PIK), 14473 Potsdam, Germany*
[3]*Department of Geosciences, Princeton University, Princeton, New Jersey 08544, USA*
[4]*ICREA and ICTA, Autonomous University of Barcelona, 08193 Bellaterra, Catalonia, Spain*
[5]*Environmental Change Research Centre, Department of Geography, University College London, London, WC1H 0AP, UK*
[6]*IFM-Geomar, 24148 Kiel, Germany*
[7]*Department of Earth Sciences, ETH Zürich, 8092 Zürich, Switzerland*
[8]*NERC Isotope Geosciences Laboratory, British Geological Survey, Keyworth, Nottingham NG12 5GG, UK*
[9]*Biogeochemistry Centre, University of Bristol, Bristol BS8 1TS, UK*

In the context of gradual Cenozoic cooling, the timing of the onset of significant Northern Hemisphere glaciation 2.7 million years ago is consistent with Milankovitch's orbital theory, which posited that ice sheets grow when polar summertime insolation and temperature are low. However, the role of moisture supply in the initiation of large Northern Hemisphere ice sheets has remained unclear. The subarctic Pacific Ocean represents a significant source of water vapour to boreal North America, but it has been largely overlooked in efforts to explain Northern Hemisphere glaciation. Here we present alkenone unsaturation ratios and diatom oxygen isotope ratios from a sediment core in the western subarctic Pacific Ocean, indicating that 2.7 million years ago late-summer sea surface temperatures in this ocean region rose in response to an increase in stratification. At the same time, winter sea surface temperatures cooled, winter floating ice became more abundant and global climate descended into glacial conditions. We suggest that the observed summer warming extended into the autumn, providing water vapour to northern North America, where it precipitated and accumulated as snow, and thus allowed the initiation of Northern Hemisphere glaciation.

To initiate and sustain the large Northern Hemisphere ice sheets of the Plio-Pleistocene ice ages, two requirements are broadly recognized. First, the more polar continental areas must be sufficiently cold for precipitation to fall as snow rather than rain and for snow and ice to survive the warm summer melting season. Second, adequate moisture must be introduced to high northern latitudes to promote the accumulation of glacial ice. In attempts to explain the initiation of the major Northern Hemisphere glaciation 2.7 million years (Myr) ago, much attention has been given to the temperature requirements of continental glaciation. The time interval between 4.5 and 3.1 Myr was dominated by a pronounced long-term minimum in the amplitude of the 41-kyr cycle in the obliquity of the Earth's rotation[1], which would have failed to produce particularly cold Northern Hemisphere summers—the key requirement posited by Milankovitch for the onset of Northern Hemisphere glaciation. During this time interval, there may have been several aborted shifts toward glaciation, for example, between 4.1–3.9 Myr and 3.5–3.3 Myr (ref. 2; Fig. 1). During the late Pliocene and early Pleistocene, a high amplitude in the obliquity cycle resulted in periods of low tilt angle, which, in turn, would have yielded periods with cold summers in the Northern Hemisphere. Thus, it has been suggested that the progressive increase in the amplitude of the obliquity cycle tipped the scale between 3.1–2.5 Myr, allowing for long-term expansion of Northern Hemisphere ice[1]. In short, our long-held view of the temperature requirement of glaciation is largely consistent with the timing of the onset of Northern Hemisphere glaciation.

However, the onset of Northern Hemisphere glaciation has proved to be inconsistent with ideas regarding the water vapour requirement[3,4]. It has been suggested that glaciation began in response to increased North Atlantic Deep Water formation and the flow of warm Gulf Stream waters into the high-latitude North Atlantic, associated with the closure of the Panama seaway[5,6]. However, recent studies show that this closure and associated changes in North Atlantic circulation occurred 4.6 Myr ago, well before the onset of intense Northern Hemisphere glaciation[4,5]. Thus, it is unknown whether and how a change in water vapour supply encouraged the initiation of intense Northern Hemisphere glaciation.

Seasonality of the modern subarctic North Pacific

The modern subarctic Pacific surface is dominated by a permanent 'halocline', or salinity-driven density gradient in the upper 300 m, that reduces exchange between the surface layer and the ocean interior[7]. Seasonal changes in the temperature of the surface mixed layer are thus only minimally buffered by the heat capacity of the ocean subsurface, resulting in a sea surface temperature (SST) that has one of the largest annual ranges of any open ocean region, with winter (February) surface ocean temperatures in the subarctic Northwest Pacific of about +1 °C, late-summer (September) temperatures of +12 °C, and a seasonal thermocline during summer and autumn[8].

This seasonal variation in the physical conditions of the subarctic Pacific leads to strong seasonality in the biological productivity of the region. Winter mixing transports nutrients from the subsurface into the euphotic zone. During spring, as the euphotic zone deepens and the mixed layer shoals, a diatom-dominated bloom begins, lasting until early summer, when most of the nutrients are consumed, silicate in particular[9,10]. However, during late summer and autumn, when the water column is most stable, a secondary biogenic bloom typically occurs, this time dominated by coccolithophores[11,12]. Alkenones accumulating in the sediments below

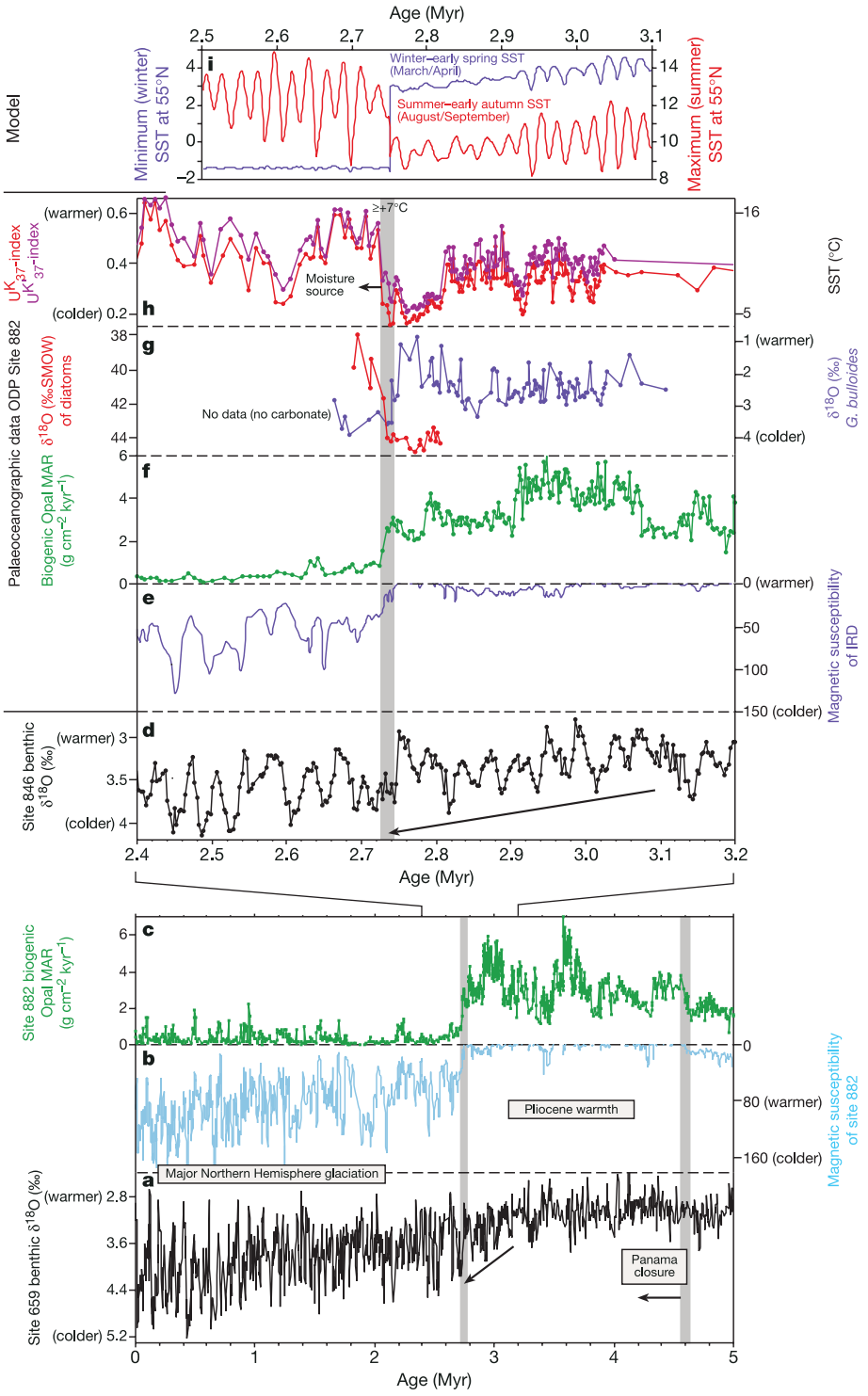

Figure 1 Palaeoceanographic data and model time series through the time interval marking the onset of major Northern Hemisphere glaciation. **a**, Increase in ice volume between 3.1 and 2.7 Myr, as indicated by benthic foraminiferal $\delta^{18}O$ from ODP Site 659, in the eastern equatorial Atlantic Ocean[34]. **b**, IRD input to the subarctic Northwest Pacific, as indicated by the increase in magnetic susceptibility at ODP Site 882 (50° 21′ N, 167° 35′ E, water depth 3,244 m) at 2.73 Myr. **c**, Drop in biogenic opal mass accumulation rates (MAR) at ODP Site 882 in the subarctic Northwest Pacific. **d**–**h**, During the time interval 3.2 to 2.4 Myr, fluctuations in ice volume as indicated by benthic foraminiferal $\delta^{18}O$ from ODP Site 846, eastern equatorial Pacific[2] (**d**), IRD at ODP Site 882 (**e**), biogenic opal MARs at ODP Site 882 (**f**), $\delta^{18}O$ in planktonic foraminifera *G. bulloides* (blue), which is interpreted to reflect mainly winter/spring SST, and $\delta^{18}O$ of large diatom species *C. marginatus* and *C. radiatus* (red), which is interpreted to reflect mainly late summer/autumn SST (**g**), and U^{K}_{37}- and $U^{K'}_{37}$-indices, which are interpreted to reflect mainly late summer/autumn SST (**h**). The range of absolute SSTs (in °C, right axis) reflect the U^{K}_{37} temperature calibration of ref. 18, which is in close agreement with that of ref. 19. **i**, CLIMBER-2 model output of minimum (blue; March/April or winter/spring) and maximum (red; August/September or summer autumn) zonally averaged Pacific SST at 55° N.

this region indicate a modern temperature of 10.1 °C, consistent with the late-summer and autumn growth of the coccolithophorids, which are among the prymnesiophytes that produce these compounds[11].

North Pacific changes 2.7 Myr ago

Before about 2.7 Myr ago, the accumulation of diatomaceous sediments in the subarctic Pacific was roughly four to five times greater than it is today (Fig. 1; ODP Site 882: 50° 21′ N, 167° 35′ E, water depth of 3,244 m). Records from both the western and eastern basins of the subarctic Pacific indicate an abrupt drop in opal accumulation rate at isotope stage G6, synchronous with the massive onset of ice-rafted debris (IRD, Fig. 1). The nearly complete consumption of silicate in the modern subarctic Pacific summertime surface and a sedimentary N isotope change across the 2.7-Myr transition conspire to indicate that the drop in opal accumulation was associated with a drop in the supply of major nutrients from the ocean interior to the surface ocean[13]. Thus, the biogeochemical data point to the development of the subarctic Pacific halocline at 2.7 Myr, closely associated with the onset of major Northern Hemisphere glaciation[13] (Fig. 1).

The close association of subarctic Pacific halocline formation with major Northern Hemisphere glaciation as well as the abrupt and dramatic nature of both changes suggest a positive feedback between the two. We have previously focused on how climate cooling increased the vertical stability of the North Pacific[13,14]. This work raised atmospheric CO_2 as the possible mechanism by which polar stratification could, in turn, cause global cooling and thus participate in a positive feedback. The sediment core data and climate model output reported here provide a more direct mechanism by which the development of the subarctic Pacific halocline set the scene for ice-sheet growth in the Northern Hemisphere.

The $\delta^{18}O$ of microfossil calcite from the planktonic foraminifer *G. bulloides* increases at 2.7 Myr by approximately 2‰ (ref. 14; Fig. 1). This has been taken to indicate a drop in SST of about 5 °C, taking ice-volume variations into account[15]. The $\delta^{18}O$ increase occurs shortly (~3 kyr) before the drop in opal accumulation and coincides with the first step in IRD increase. Poor preservation makes such a foraminifera-derived reconstruction difficult in these nearly carbonate-free sediments, especially after the 2.7-Myr transition. Nevertheless, the sharp increase in IRD across the transition and the evidence from other regions[16] confirm that the overall sense of change at 2.7 Myr was a dramatic cooling.

We have measured alkenone unsaturation ratios[17–22] (U^{K}_{37} and $U^{K}_{37}{}'$) across the 2.7-Myr transition at ODP Site 882, to provide an additional constraint on surface temperature changes in the subarctic North Pacific. Prymnesiophytes, including the coccolithophorids, produce the long-chain alkenones that are used in this temperature reconstruction. As phytoplankton, these organisms are concentrated in the upper euphotic zone of polar waters, whereas *G. bulloides* can live at a variety of depths and also forms a gametogenic crust in the subsurface. Moreover, coccolithophorids tend to bloom in the middle to late summer in the western subarctic Pacific, after the diatom bloom[9–12], whereas foraminiferal production tends to follow the productivity of the entire phytoplankton pool and thus is at a maximum in the spring[9,10]. For these reasons, significant differences should be expected between alkenone- and foraminiferal-based temperature reconstructions. Even with this expectation, the alkenone-derived temperature change is in surprising contrast to the indicators of cooling at the 2.7-Myr transition: the alkenone data indicate a warming of ≥7 °C across the transition (Fig. 1).

Given this unexpected result, possible sources of artefact must be considered. The alkenone content of these old, high-latitude sediments is quite low, requiring the use of a high-sensitivity gas chromatography-chemical ionization mass spectrometry (GC-CIMS) method for measurement of the degree of alkenone unsaturation[23] (see Supplementary Information). Diagenesis and changes in light and nutrient conditions are not expected to bias the unsaturation ratios to the degree that would be required to explain the transition at 2.7 Myr (refs 24, 25). A recent concern is that alkenones can be transported laterally, associated with fine sediments, and can perhaps be remobilized from ancient sediments[26]. This is an unlikely concern for the sediments of ODP Site 882. Sediment transport in the region is, if anything, from the North, and there is no evidence for a radical change in lateral transport at the 2.7-Myr transition. For remobilization and subsequent incorporation of alkenones from older sediments to have caused the apparent decrease in U^{K}_{37} at the 2.7-Myr transition, extremely old sediments would need to be eroded to produce such a 'warm' U^{K}_{37} signature. This assumption is not supported by the composition of the coccolith assemblage, which is dominated by coccoliths typical/indicative of the time period analysed (mainly gephyrocapsids and reticulofenestrids).

The alkenone evidence for post-2.7-Myr summertime warming is corroborated by the $\delta^{18}O$ of the silica frustules produced by large (75–150 μm) autumn-living subarctic North Pacific diatom species (*Coscinodiscus marginatus* and *C. radiatus*, see Supplementary Information). Their $\delta^{18}O$ decreases by approximately 5‰ across the 2.7-Myr transition (Fig. 1), indicating some combination of warming and freshening in the late-summertime/autumn surface. Development of the full modern halocline in the subarctic Pacific at 2.7 Myr can explain only ~1‰ of this $\delta^{18}O$ decrease[8], whereas one would expect ice volume to have caused a global ocean $\delta^{18}O$ increase of ~0.5‰ (ref. 2). This leaves a ~4.5‰ decrease to be explained by late-summertime/autumn sea surface warming. Published coefficients for the dependence of diatom silica $\delta^{18}O$ on temperature range from 0.2‰ to 0.5‰ per °C (refs 27–29). Thus, the diatom $\delta^{18}O$ data appear to require a warming of ≥9 °C at 2.7 Myr, which is similar to the warming estimate from the alkenones. Although significant uncertainties remain in the use of diatom $\delta^{18}O$, they are completely different from those that apply to the alkenones. In particular, lateral transport or exhumation from older sediments are not plausible concerns for these large and extremely well-preserved diatoms (see Supplementary Information).

A link between stratification and seasonality

Despite the initially counterintuitive nature of these results, warming is completely consistent with the development of the subarctic Pacific halocline at 2.7 Myr. Because the halocline acts to reduce exchange between the surface and ocean interior, the development of the halocline at 2.7 Myr should have caused the seasonal variation of surface ocean temperature to reflect more fully the seasonal cycle in insolation and air temperature. That is, upon stratification, the seasonal variation in surface temperature should have increased toward the ~11 °C range that characterizes the modern subarctic Pacific. The U^{K}_{37}-index reflects the SST maximum that coincides with the late-summer/autumn coccolith bloom, and the diatoms analysed here also grow at the surface during the late summer[10]. By contrast, the foraminiferal calcite is biased to record the spring diatom bloom and is also strongly influenced by the temperature of the shallow subsurface through growth below the mixed layer and the formation of gametogenic crust. Consequently, the apparent paradox between the cooling at 2.7 Myr as indicated by the planktonic foraminifera $\delta^{18}O$ and the warming as indicated by the U^{K}_{37}-index and diatom $\delta^{18}O$ is best interpreted as an expression of the amplified seasonal contrast that should have been expected from the development of the permanent halocline at that time.

The high heat capacity of sea water causes surface waters to remain warm into the autumn and cool into the spring. Stratification of the subarctic Pacific will decrease the thermal inertia of the upper ocean and thus reduce the phase lag between land and ocean temperature. However, the amplification of the seasonal cycle

should overwhelm this effect, so that stratification will cause the subarctic Pacific surface to be significantly warmer than the land further into the autumn.

Such an enhanced temperature contrast with continental climate, which responds rapidly to seasonal insolation changes, is well suited for driving glaciation in North America. The subarctic Pacific is a dominant source of water vapour to boreal North America[30], and warmer SSTs in the autumn would cause a larger fraction of the water vapour delivery to occur when continental climate is cold enough for snow to accumulate. In this way, the stratification of the subarctic Pacific would allow for adequate water vapour supply to feed glaciers when global climate cooling would otherwise drive a decrease in water vapour transport and limit ice-sheet growth. Thus, the obliquity minimum within isotope stage G6 at 2.7 Myr may have succeeded in beginning the age of intense Northern Hemisphere glaciations specifically because it triggered the development of the subarctic Pacific halocline, which then continued to provide water vapour to boreal North America even as the globally averaged atmosphere became colder and drier.

North Pacific seasonality and glaciation

To test the links among subarctic Pacific stratification, SST and ice-sheet growth, we carry out a suite of experiments with CLIMBER-2, an Earth system model of intermediate complexity[31,32]. To control stratification, we vary the freshwater input into the subarctic North Pacific region. If this input is reduced from modern forcing by 0.2 Sv (~20% of the total precipitation over the North Pacific), the model comes to equilibrium with a 'destratified' subarctic Pacific that lacks its modern halocline. An increase in freshwater input is unlikely to have been the specific cause of subarctic Pacific stratification at 2.7 Myr (ref. 13); it merely represents a simple model strategy for changing polar stratification[31] (see also Supplementary Information).

The 'destratified' and 'stratified' equilibria differ in ways that are consistent with their representation of pre- and post-2.7 Myr conditions, respectively. Relative to the 'destratified' equilibrium, the modern equilibrium maintains much colder winter and spring SSTs in the subarctic Pacific and has significant seasonal sea-ice cover, which the 'destratified' equilibrium lacks. Despite the overall cooling associated with the modern equilibrium, late-summer and autumn SST is actually warmer in this modern equilibrium, which we explain above as the result of reduced thermal inertia associated with stratification. Relative to the destratified state, the cold spring in the stratified state reduces spring and summer snowmelt (Fig. 2a, b). At the same time, the warm autumn SST of the stratified state maintains the moisture supply to North America (Fig. 2c, d) despite annually averaged cooling.

To assess the significance of the differences between the stratified and destratified states for the build-up of ice sheets in the Northern Hemisphere, we performed additional experiments using an extreme orbital configuration called 'cold orbit'. A high-resolution snow pack model coupled to CLIMBER-2 was used to diagnose the area of permanent snow cover, which can be considered as a minimum footprint for the ice sheets. For the modern climate state (stratified North Pacific) and the 'cold orbit', a large area of North America is perennially covered by snow (Fig. 3b). In contrast, with a destratified North Pacific, the area of perennial snow cover is restricted to the Arctic archipelago and small mountainous areas (Fig. 3a). Growth of the ice sheet provides an additional positive feedback, which explains part of the large temperature difference between the stratified and destratified North Pacific climate states (Fig. 3b, see also Supplementary Information).

A time-evolving experiment simulates the development of stratification at 2.7 Myr (Fig. 1i). The experiment begins at 3.1 million years ago (Fig. 1i) from the destratified state and gradually increases the freshwater flux to the subarctic Pacific at a constant rate of 0.2 Sv per million years. The simulation also includes orbital parameter variation[1]. At 2.75 Myr, stratification sets in, winter/springtime (March/April) subarctic Pacific SST drops by ~5 °C, and summertime/autumn (August/September) SST increases by ~3 °C. The timing of the gradual freshwater increase has been optimized to yield stratification at 2.7 Myr. However, the abrupt development of stratification from the gradual change in freshwater input was a natural response of the model, indicating that a 2.7-Myr stratification event may have been a threshold response to a gradual change in forcing.

Previous work on the connection between water vapour supply and Northern Hemisphere glaciation has focused on the North Atlantic. The connection between deep convection and meridional heat transport in the North Atlantic has represented a central motivation for this focus[33]. It is obvious that the North Pacific, a large oceanic region that is upstream of North America in

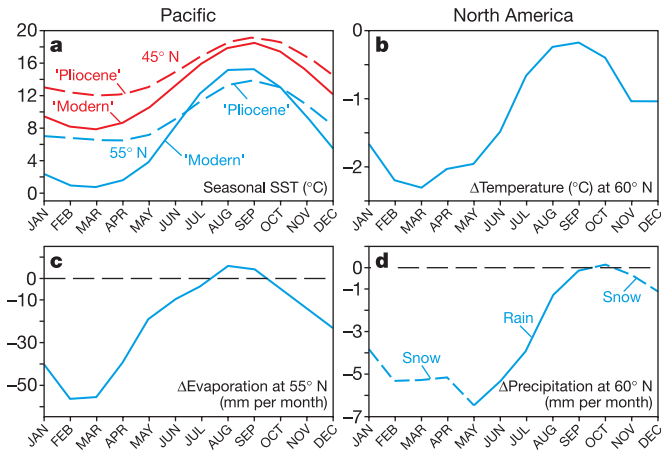

Figure 2 Output for two equilibrium states of the CLIMBER-2 Earth system model. **a**, Seasonal variation in North Pacific SST at 55° N (blue) and 45° N (red). The solid lines correspond to the 'modern' (stratified) equilibrium, the dashed lines to the 'Pliocene' (unstratified) equilibrium state. **b**–**d**, 'Modern' minus 'Pliocene' differences in seasonal variation of temperature (**b**) and precipitation (as snow and rain) zonally averaged over Northern America at 60° N (**d**), and evaporation from the North Pacific at 55° N (**c**).

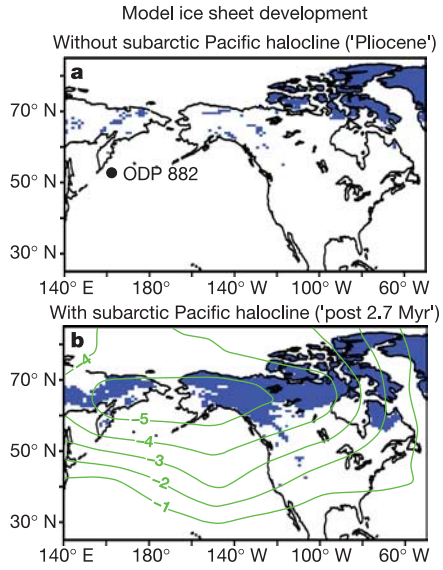

Figure 3 Simulated area of permanent snow cover (shaded) for the 'cold orbit' configuration in the destratified (**a**) and stratified (**b**) equilibria. **b**, Isolines (green) show differences in annual surface air temperature between climate states corresponding to stratified and destratified equilibria under the 'cold orbit' configuration.

atmospheric circulation, could play a critical role in the development of Northern Hemisphere glaciation. Ironically, it was the isolation of the subarctic Pacific surface from the ocean interior that set the stage for major Northern Hemisphere glaciation at 2.7 Myr. □

Received 18 October; accepted 30 December 2004; doi:10.1038/nature03332.

1. Berger, A. & Loutre, M. F. Insolation values for the climate of the last 10 million years. *Quat. Sci. Rev.* **10,** 297–317 (1991).
2. Shackleton, N. J., Hall, M. & Pate, D. Pliocene stable isotope stratigraphy of Site 846. *Proc. ODP Sci. Res.* **138,** 337–357 (1995).
3. Cane, M. A. & Molnar, P. Closing the Indonesian seaway as a precursor to East African aridification around 3–4 million years ago. *Nature* **411,** 157–162 (2001).
4. Ravelo, A. C., Andreasen, D. H., Lyle, M., Olivarez Lyle, A. & Wara, M. W. Regional climate shifts caused by gradual cooling in the Pliocene epoch. *Nature* **429,** 263–267 (2004).
5. Haug, G. H. & Tiedemann, R. Effect of the formation of the Isthmus of Panama on Atlantic Ocean thermohaline circulation. *Nature* **393,** 673–676 (1998).
6. Keigwin, L. D. Isotope paleoceanography of the Caribbean and east Pacific: Role of Panama uplift in late Neogene time. *Science* **217,** 350–353 (1982).
7. Gargett, A. E. Physical processes and the maintenance of nutrient-rich euphotic zones. *Limnol. Oceanogr.* **36,** 1527–1545 (1991).
8. Levitus, S. & Boyer, T.P. *World Ocean Atlas 1994* Vol. 4 *Temperature* 129 (NOAA Atlas NESDIS, National Oceanographic Data Center, Silver Spring, USA, 1994).
9. Wong, C. S., Whitney, F. A., Tsoy, I. & Bychkov, A. in *Global Fluxes of Carbon and its Related Substances in the Coastal Sea–Atmosphere System* (eds Tsunogai, S. *et al.*) 339–344 (Proc. 1994 Sapporo IGBP Symp., M&J International, Yokohama, Japan, 1995).
10. Takahashi, K. Seasonal fluxes of pelagic diatoms in the subarctic Pacific, 1982–1983. *Deep-Sea Res.* **33,** 1225–1251 (1986).
11. Ohkouchi, N., Kawamura, K., Kawahata & Okada, H. Depth ranges of alkenone production in the central Pacific Ocean. *Glob. Biogeochem. Cycles* **13,** 695–704 (1999).
12. Pagani, M., Freeman, K. H., Ohkouchi, N. & Caldeira, K. Comparison of water column [CO_2aq] with sedimentary alkenone-based estimates: A test of the alkeonone-CO_2 proxy. *Paleoceanography* **17**(4), doi:10.1029/2002PA000756 (2002).
13. Sigman, D. M., Jaccard, S. & Haug, G. H. Polar ocean stratification in a cold climate. *Nature* **428,** 59–63 (2004).
14. Haug, G. H., Sigman, D. M., Tiedemann, R., Pedersen, T. F. & Sarnthein, M. Onset of permanent stratification in the subarctic Pacific Ocean. *Nature* **40,** 779–782 (1999).
15. Maslin, M. A. *et al.* Northwest Pacific Site 882: The initiation of Northern Hemisphere glaciation. *Proc. ODP Sci. Res.* **145,** 315–333 (1995).
16. Shackleton, N. J. *et al.* Oxygen isotope calibration of the onset of ice-rafting and history of glaciation in the North Atlantic region. *Nature* **307,** 620–623 (1984).
17. Brassell, S. C., Eglinton, G., Marlowe, I. T., Pflaumann, U. & Sarnthein, M. Molecular stratigraphy: A new tool for climatic assessment. *Nature* **320,** 129–133 (1986).
18. Prahl, F. G. & Wakeham, S. G. Calibration of unsaturation patterns in long-chain ketone compositions for palaeotemperature assessment. *Nature* **330,** 367–369 (1987).
19. Müller, P. J., Kirst, G., Ruhland, G., von Stroch, I. & Rosell-Mele, A. Calibration of the alkenone paleotemperature index $U^{K}_{37'}$ based on core-tops from the eastern South Atlantic and the global ocean (60°N-60°S). *Geochim. Cosmochim. Acta* **62,** 1757–1772 (1998).
20. Sachs, J. P. *et al.* Alkenones as paleoceanographic proxies. *Geochem. Geophys. Geosyst.* **1,** 1–13 (2000).
21. Volkman, J. K. Ecological and environmental factors affecting alkenone distributions in seawater and sediments. *Geochem. Geophys. Geosyst.* **1,** 1–12 (2000).
22. Bard, E. Comparison of alkenone estimates with other paleotemperature proxies. *Geochem. Geophys. Geosyst.* **2,** 1–12 (2001).
23. Rosell-Mele, A., Carter, J., Parry, A. & Eglinton, G. Novel procedure for the determination of the $U^{k}_{37'}$ in sediment samples. *Anal. Chem.* **67,** 1283–1289 (1995).
24. Grimalt, J. O. *et al.* Modification of the C_{37} alkenone and alkenoate composition in the water column and sediments: Possible implications for sea surface temperature estimates in paleoceanography. *Geochem. Geophys. Geosyst.* **1,** 1–20 (2000).
25. Prahl, F. G., Wolfe, G. V. & Sparrow, M. A. Physiological impacts on alkenone paleothermometry. *Paleoceanography* **18**(1052), doi:10.1029/2002PA000853 (2003).
26. Ohkouchi, N., Eglinton, T. I., Keigwin, L. D. & Hayes, J. M. Spatial and temporal offsets between proxy records in a sediment drift. *Science* **298,** 1224–1227 (2002).
27. Juillet-Leclerc, A. & Labeyrie, L. Temperature dependence of the oxygen isotope fractionation between diatom silica and water. *Earth Planet. Sci. Lett.* **84,** 69–74 (1987).
28. Shemesh, A., Charles, C. D. & Fairbanks, R. G. Oxygen isotopes in biogenic silica: global changes in ocean temperature and isotopic composition. *Science* **256,** 1434–1436 (1992).
29. Brandriss, M. E., O'Neil, J. R., Edlund, M. B. & Stoermer, E. F. Oxygen isotope fractionation between diatomaceous silica and water. *Geochim. Cosmochim. Acta* **62,** 1119–1125 (1998).
30. Koster, R. *et al.* Global sources of local precipitation as determined by the NASA/GISS GCM. *Geophys. Res. Lett.* **13,** 121–124 (1986).
31. Ganopolski, A., Rahmstorf, S., Petoukhov, V. & Claussen, M. Simulation of modern and glacial climates with a coupled global model of intermediate complexity. *Nature* **391,** 351–356 (1998).
32. Petoukhov, V. *et al.* CLIMBER-2: A climate system model of intermediate complexity. Part I: Model description and performance for present climate. *Clim. Dyn.* **16,** 1–17 (2000).
33. Broecker, W. S. Thermohaline circulation, the Achilles heel of our climate system: will man-made CO_2 upset the current balance? *Science* **278,** 1582–1588 (1997).
34. Tiedemann, R., Sarnthein, M. & Shackleton, N. J. Astronomic timescale for the Pliocene Atlantic $\delta^{18}O$ and dust flux records of ODP Site 659. *Paleoceanography* **9,** 619–638 (1994).

Supplementary Information accompanies the paper on **www.nature.com/nature**.

Acknowledgements We thank M. Sarnthein, H. Thierstein, M. Zhao and S. Honjo for discussions. J. Barron, J. Onodera and K. Takahashi provided insight on diatoms *C. marginatus* and *C. radiatus* and their seasonal fluxes in the North Pacific, and H. Sloane helped with the diatom $\delta^{18}O$ analyses. We thank the Ocean Drilling Program (ODP) and the scientific party and crew of ODP Leg 145 for their efforts in the drilling of Site 882. This work was supported by the Deutsche Forschungsgemeinschaft (DFG), Schweizer Nationalfonds (SNF), the US National Science Foundation (NSF) and BP and the Ford Motor Company through the Princeton University Carbon Mitigation Initiative.

Competing interests statement The authors declare that they have no competing financial interests.

Correspondence and requests for materials should be addressed to G.H.H. (haug@gfz-potsdam.de).